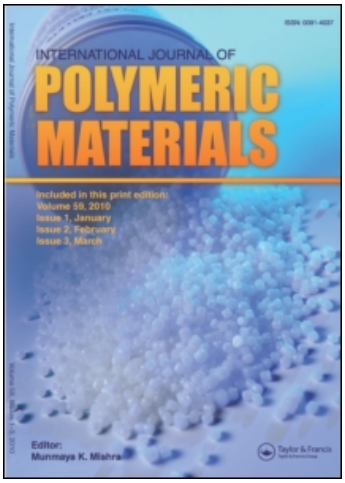

International Journal of Polymeric Materials
Publication details, including instructions for authors and subscription information:
http://www.informaworld.com/smpp/title~content=t713647664

Computer Simulation of Kinetics of Coil-Stretched Chain Transition in Elongational Flow

A. A. Darinskii[a]; A. V. Lyulin[a]; M. G. Saphiannikova[a]
[a] Institute of Macromolecular Compounds, Russian Academy of Sciences, St. Petersburg, Russia

To cite this Article Darinskii, A. A. , Lyulin, A. V. and Saphiannikova, M. G.(1993) 'Computer Simulation of Kinetics of Coil-Stretched Chain Transition in Elongational Flow', International Journal of Polymeric Materials, 22: 1, 15 — 24
To link to this Article: DOI: 10.1080/00914039308012053
URL: http://dx.doi.org/10.1080/00914039308012053

Intern. J. Polymeric Mater., 1993, Vol. 22, pp. 15–24
Reprints available directly from the publisher
Photocopying permitted by license only

Printed in Malaysia

Computer Simulation of Kinetics of Coil-Stretched Chain Transition in Elongational Flow

A. A. DARINSKII, A. V. LYULIN, and M. G. SAPHIANNIKOVA

Institute of Macromolecular Compounds, Russian Academy of Sciences, 31 Bol'shoi pr., St. Petersburg 199004, Russia

The Brownian dynamics technique is used to simulate the behavior of a polymer chain in an elongational flow. A macromolecule is represented by dumbbell with conformation-dependent friction coefficient. Equilibrium and kinetic properties of the chain are studied. The effective potential approximation is shown to be quite appropriate for the description of the chain distribution function. The transition times through the effective potential barrier are in a good agreement with the prediction of the Kramers theory. The S-shaped curve for the extension ratio of the dumbbell as a function of the velocity gradient is observed when simulation times are comparable with the transition times.

KEY WORDS Dumbbell model, conformation-dependent friction coefficient, elongational flow, effective potential, kinetics.

1. INTRODUCTION

It is well known that the coil-stretched chain transition of flexible polymers in an elongational flow is observed when the critical value of the velocity gradient $\dot{\epsilon}$ is attained.[1–3] The correct mathematical description of this phenomenon is rather a complicated problem. To simplify it one generally uses the dumbbell model for polymer chain. However, even for the dumbbell model the problem cannot be solved analytically without some approximations. The solution of the problem should contain the distribution function for chain conformations at different velocity gradients and different chain parameters. De Gennes has used an one-dimensional approximation[4] and obtained the distribution function for extension ratios β. This function has two peaks in the region of velocity gradients near the critical value $\dot{\epsilon}_{cr}$. These results allowed him to introduce an effective potential for the chain and consider the chain motion in an elongational flow as a motion in the field of this potential. In Reference 5 the spatial distribution function has been obtained for the dumbbell model. Contrary to de Gennes, they used *ab initio* the effective potential approximation in which the nonpotential part of hydrodynamic force is neglected.

Despite the progress achieved[5] in comparison with de Gennes' results[4] the question remains unsolved if the effective potential description is correct. It should be noted that in this case it is a fundamental problem, rather than the problem of accurate description. The system consisting of a stretched macromolecule in an elongational flow is a nonequilibrium dissipative system and the applicability of the equilibrium statistical mechanics to this

system is not obvious. A similar question arises if we consider the transition kinetics of the macromolecule between the coiled and stretched states as a Brownian motion in the external effective potential.[6] To answer these questions the motion of dumbbell model in an elongational flow without any approximations should be simulated, which has been performed in our study using the Brownian dynamics technique.

Another interesting problem is connected with the S-shaped curve for the extension ratio of macromolecules as a function of the velocity gradient $\dot{\epsilon}$. Such a curve has been obtained by de Gennes with the help of self-consistency approximation,[4] where the elastic constant and friction coefficient depend on the root-mean-square extension of the dumbbell at the current time. The de Gennes result was criticized in the work of Bird *et al.*[7] The criticism was based on numerical solution of the diffusion equation for the dumbbell model by Galerkin's method. Bird did not obtain the S-shaped curve and "felt strongly persuaded that S-shaped curves in the dumbbell calculations must result from the mathematical approximation made."[7] Therefore the problem of the S-shaped curve has also been considered in present work.

This paper is organized as follows. Section 2 briefly outlines the effective potential approximation of Brestkin *et al.*[5] Section 3 describes the model and simulation technique. Finally the results obtained and their discussion are presented in Section 4.

2. EFFECTIVE POTENTIAL APPROXIMATION

A flexible macromolecule consisting of N identical segments of length A and friction coefficient ζ_s is represented by a viscoelastic dumbbell with elastic constant $E(\beta)$ and beads friction coefficient $\zeta_b(\beta)$ both depending on the extension ratio β. Here $\beta = h/NA$, $h = |\boldsymbol{h}|$, $\boldsymbol{h}$ is end-to-end vector of the dumbbell.

The dumbbell is located in elongational flow with velocity gradient tensor:

$$\hat{\boldsymbol{K}} = \dot{\epsilon} \begin{pmatrix} 1 & 0 & 0 \\ 0 & -1/2 & 0 \\ 0 & 0 & -1/2 \end{pmatrix}. \tag{1}$$

It was shown[8] that for steady-state elongational flow the diffusion equation for dumbbell model is reduced to force balance equation:

$$\boldsymbol{F}_s + \boldsymbol{F}_{el} + \boldsymbol{F}_d = 0, \tag{2}$$

where $\boldsymbol{F}_s = [\zeta_b(\beta)/2]\hat{\boldsymbol{K}}\boldsymbol{h}$ is the hydrodynamic force, $\boldsymbol{F}_{el} = -(3kT/N)E(\beta)\boldsymbol{h}$ is the elastic force, $\boldsymbol{F}_d = -kT\nabla \ln \Psi(\boldsymbol{h})$ is the smoothed up Brownian motion force. Here $\Psi(\boldsymbol{h})$ is the distribution function for end-to-end vector $\boldsymbol{h}$.

This equation cannot be solved analytically for conformation-dependent friction coefficient $\zeta_b(\beta)$ since $\mathrm{rot}\,\boldsymbol{F}_s \neq 0$. The approximation used in Reference 5 consisted in the replacing of the total hydrodynamic force $\boldsymbol{F}_s$ by its potential part $\hat{\boldsymbol{F}}_s$. Then only one scalar equation remains to be solved in the spherical coordinate system (h, θ, φ) for given θ, φ:

$$kT\frac{\partial \ln \Psi(\boldsymbol{h})}{\partial h} = \hat{F}_{sh} + F_{elh}, \tag{3}$$

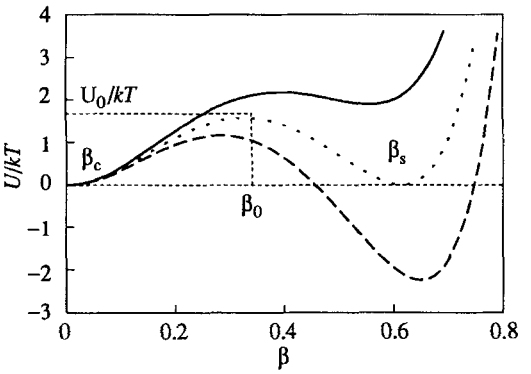

FIGURE 1 The effective potential $U(\beta)$ for $N = 100$ at $\theta = 0°$: $\dot{\epsilon} < \dot{\epsilon}_{cr}$ (solid curve), $\dot{\epsilon} = \dot{\epsilon}_{cr}$ (dotted curve), $\dot{\epsilon} > \dot{\epsilon}_{cr}$ (dashed curve).

where $\hat{F}_{sh}$ and F_{elh} are the projections of hydrodynamic and elastic forces on flow axis.

The stationary distribution function can be obtained by integrating this equation over h:

$$\Psi(h, \theta, \varphi) = \text{const} \exp\left(\frac{1}{kT}\int_0^h \left[\hat{F}_{sh}(h, \theta, \varphi) + F_{elh}(h, \theta, \varphi)\right] dh\right). \quad (4)$$

The function

$$U(h) = -\int_0^h \left(\hat{F}_{sh} + F_{elh}\right) dh \quad (5)$$

can be interpreted as effective potential for the system under consideration. To obtain the dependence $U(\beta)$ one should choose the concrete form for dependencies $E(\beta)$ and $\zeta_b(\beta)$. At present time a number of different forms has been used.[9–11] In the paper of Brestkin *et al.*[12] the following expressions have been proposed:

$$E(\beta) = 1 + \frac{\beta^2}{3(1-\beta)} \quad (6)$$

$$\zeta_b(\beta) = \begin{cases} \zeta_b^0, & \text{at } \beta \le \beta_0 \\ \zeta_b^0\left(\dfrac{N^{1/2}}{\ln N}\dfrac{1+\beta}{2} - B\exp(-5\beta)\right) & \text{at } \beta \ge \beta_0, \end{cases} \quad (7)$$

where

$$B = \left(\frac{N^{1/2}}{\ln N}\frac{1+\beta_0}{2} - 1\right)\exp(5\beta_0), \qquad \beta_0 = \frac{1}{N^{1/2}}.$$

In Figure 1 the effective potential curves $U(\beta)$ at $\theta = 0°$ calculated with the help of dependencies (6) and (7) are presented for $N = 100$ and different values of velocity gradient $\dot{\epsilon}$. One can see that in some region of $\dot{\epsilon}$ the potential curve has two minima corresponding to the coiled and stretched states of the dumbbell. The value $\dot{\epsilon}_{cr}$ at which both minima have equal depths (dotted curve in Figure 1) are referred as a critical value of velocity gradient.

TABLE I
The optimal time steps Δt in units of $\zeta_b^0 \lambda$

N	50	100	150	200	250
Δt	0.0004	0.001	0.0025	0.004	0.015

λ is the relaxation time of the dumbbell at equilibrium.

3. MODEL AND SIMULATION TECHNIQUE

For simulation by the Brownian dynamics technique we have chosen the same dumbbell model as Brestkin *et al.*[12] The motions of the dumbbell beads are described by the Langevin equations:

$$\zeta_b(\beta)[\hat{\boldsymbol{K}}\boldsymbol{r}_i(t) - \dot{\boldsymbol{r}}_i] + (-1)^i \boldsymbol{F}_{el} + \boldsymbol{F}_{d_i} = 0 \qquad i = 1, 2 \tag{8}$$

where $\boldsymbol{r}_i(t)$ is the position vector of i-th dumbbell bead at time t, $\dot{\boldsymbol{r}}_i$ is its instantaneous velocity, $\boldsymbol{F}_{d_i}$ is random force to which i-th bead is exposed. In finite difference form this equation can be written as follows:

$$\boldsymbol{r}_i(t + \Delta t) = \boldsymbol{r}_i(t) + \frac{\Delta t}{\zeta_b(\beta)} \left[\zeta_b(\beta)\hat{\boldsymbol{K}}\boldsymbol{r}_i(t) + (-1)^i \boldsymbol{F}_{el} + \boldsymbol{F}_{d_i}\right], \tag{9}$$

where Δt is time step, $\boldsymbol{r}_i(t + \Delta t)$ is the position vector of i-th bead at time $t + \Delta t$. The random force $\boldsymbol{F}_{d_i}$ is completely characterized by the first two momenta:

$$\langle \boldsymbol{F}_{d_i} \rangle = \zeta_b(\beta) \nabla_i \frac{kT}{\zeta_b(\beta)} \tag{10}$$

$$\langle \boldsymbol{F}_{d_i}^2 \rangle = \frac{2kT\zeta_b(\beta)}{\Delta t}. \tag{11}$$

The mean value of random force is not equal to zero. It was shown[13] that this term of random force in Langevin equation should be cased when models with a conformation-dependent friction coefficient (or, in general, conformation-dependent diffusion matrix) are considered.

Langevin equation (9) was solved numerically on IBM PC AT-386(387). To make Equation (9) dimensionless and convenient for numerical work, all the parameters were expressed in the units of length A, energy kT and time $\lambda_0 = \zeta_s A^2/kT$, where A is the value of the segment length and ζ_s is the segment friction constant of a macromolecule. To determine the optimal integration rule and the optimal values of the time step we have simulated previously the one-dimensional dumbbell model. The dumbbell motion in this case is described by one scalar equation instead of vector Equation (9). Since in this case the exact solution of Equation (2) is known the correctness of simulation procedure can be checked. The optimal integration rule is proved to be trapezoidal with one iteration and initial step made according to the Euler rule. The time steps presented in Table I turned out to be optimal for our computational resources.

The simulations were performed in two parts. In the first part the stationary situation was studied for the case when the effective potential minima have equal depths. In the second part the nonstationary situation for different velocity gradients $\dot{\epsilon}$ was examined.

TABLE II
The critical values of velocity gradient $\dot{\epsilon}_{cr}$

N	50	100	150	200	250
$\dot{\epsilon}_{cr}$, s^{-1}	1.26×10^{-3}	3.82×10^{-4}	1.87×10^{-4}	1.12×10^{-4}	7.52×10^{-5}
$\dot{\epsilon}_{cr}\lambda$	0.445	0.382	0.344	0.317	0.297

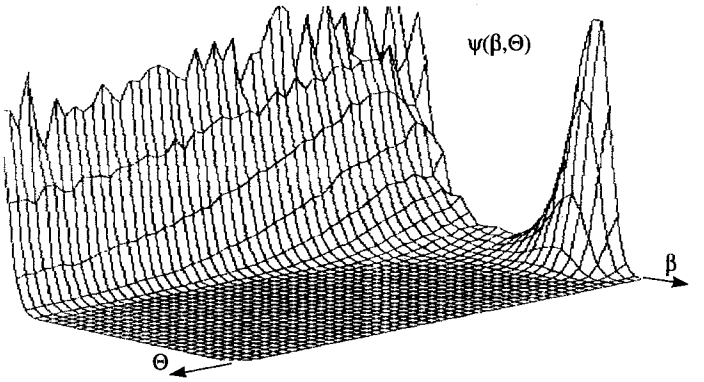

FIGURE 2 The two-dimensional distribution function $\Psi(\beta, \theta)$ for $N = 150$ at $\dot{\epsilon} = \dot{\epsilon}_{cr}$.

4. RESULTS AND DISCUSSION

Stationary case

As was mentioned in Section 2 the effective potential at the critical value of the velocity gradient $\dot{\epsilon}_{cr}$ has two minima with equal depths at β_c and at β_s corresponding to coiled and to stretched states and separated by a potential barrier of height U_0 (see Figure 1). We simulated the motion of the dumbbell model with the parameters $N = 50$, 100, 150, 200, and 250 at corresponding $\dot{\epsilon}_{cr}(N)$ (see Table II). During the simulation time, a number of transitions through a potential barrier $U_0(N)$ were observed. Simulations were performed until the total number of transitions between coiled and stretched states reached 100 for every N.

We used the simulation data to construct the distribution function $\Psi(\beta, \theta)$ and probability $P(\beta)$ to find the dumbbell within the range $\Delta\beta$ about β:

$$P(\beta) = \int_0^{\pi} \sin\theta' \mathrm{d}\theta' \int_{\beta}^{\beta+\Delta\beta} \Psi(\beta', \theta')\beta'^2 \mathrm{d}\beta',$$

where $\Delta\beta = 0.01$. In Figure 2 the example of simulated two-dimensional function $\Psi(\beta, \theta)$ is presented for $N = 150$. One can see that in the stretched state the dumbbells do not deviate significantly from the flow axis, as for the small extension ratios the random distribution of end-to-end vector $\boldsymbol{h}$ relative to flow axis is observed.

The simulation results were compared with analytical calculations performed in the effective potential approximation.[5] For $\Psi(\beta, \theta)$ there is a rather good agreement between experimental and theoretical results except for the region near β_s at small θ (see Figure 3). In this region the values of $\Psi(\beta, \theta)$ obtained analytically are smaller than those obtained

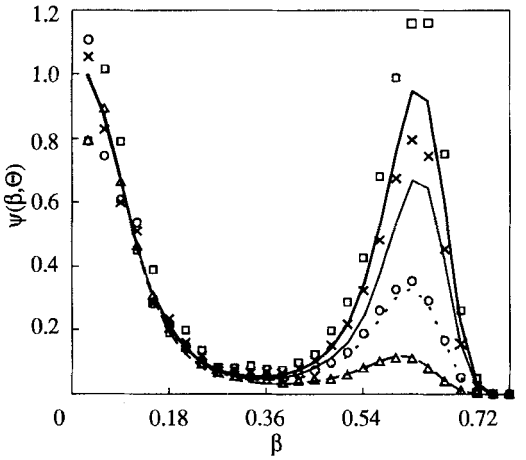

FIGURE 3 The distribution function $\Psi(\beta, \theta)$ for $N = 150$ and $\dot{\epsilon} = \dot{\epsilon}_{cr}$. The analytical results: $\theta = 1°$ (bold solid curve), $\theta = 3°$ (solid curve), $\theta = 5°$ (dotted curve), $\theta = 7°$ (dashed curve). The simulation results: $\theta = 1°$ (□), $\theta = 3°$ (×), $\theta = 5°$ (○), $\theta = 7°$ (△).

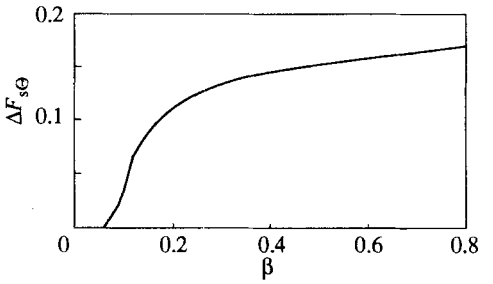

FIGURE 4 The relative difference $\Delta F_{s\theta}$ between θ-projection $F_{s\theta}$ of hydrodynamic force and its potential part $\tilde{F}_{s\theta}$ as a function of extension ratio β for $N = 150$.

at simulation. This difference, in our opinion, is a consequence of the effective potential approximation. As mentioned above, the effective potential approximation underestimates the θ-projection of the hydrodynamic force $\boldsymbol{F}_s$ (see Figure 4) that tends to align the dumbbells along the flow axis. The underestimation increases with the dumbbell extension due to the increase of friction coefficient $\zeta_b(\beta)$. The difference between analytical and simulation results can be clearly seen in Figure 5 where the angular dependence of $\Psi(\beta, \theta)$ at $\beta = \beta_s$ is shown. This difference in the region near β_s can also be observed for $P(\beta)$ (Figure 6). We can conclude that the effective potential approximation is quite appropriate over all phase space except the small region around stretched state. Even for this region, however, the maximal deviation does not exceed 20%.

Therefore we can answer affirmatively the question posed in the introduction concerning the applicability of the equilibrium statistics to the dissipative system considered here. Another question is concerned with the kinetic properties. Figure 2 shows that there is only one reaction coordinate in our system: the dumbbells must previously draw up along the flow axis, thereafter they can be stretched by the flow. Thus the barrier separating the coiled and stretched states is close to one-dimensional barrier. If transitions of the dumbbell

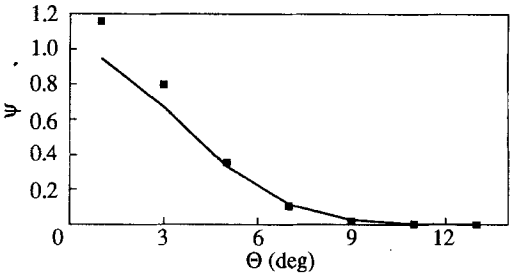

FIGURE 5 The analytical (solid curve) and simulation (■) distribution function $\Psi(\beta, \theta)$ for $N = 150$ at $\beta = \beta_s$ and $\dot{\epsilon} = \dot{\epsilon}_{cr}$.

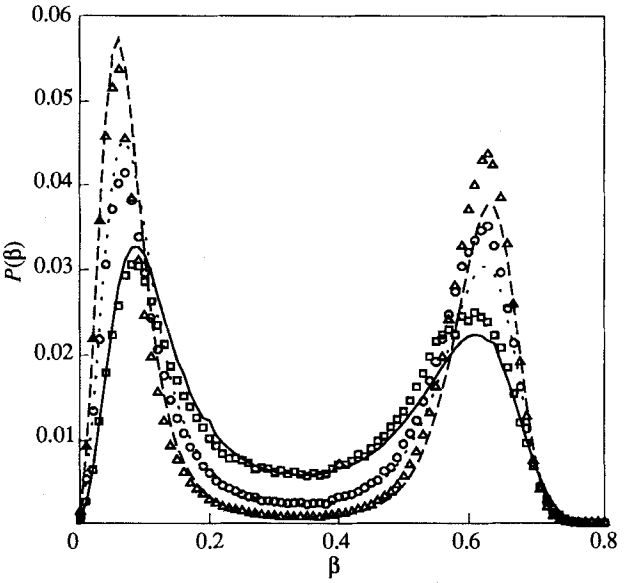

FIGURE 6 The probability function $P(\beta)$. The analytical results: $N = 100$ (solid curve), $N = 150$ (dotted curve), and $N = 200$ (dashed curve). The simulation results: $N = 100$ (□), $N = 150$ (○), and $N = 200$ (△).

between these states could be considered as the Brownian motion over the one-dimensional potential barrier the Kramers theory could be applied:[14]

$$\tau_{c\to s} = \frac{\pi}{2kT}\frac{\zeta_b(\beta_0)}{(K_c K_0)^{1/2}}\exp\left(\frac{U_0}{kT}\right) \tag{12}$$

$$\tau_{s\to c} = \frac{\pi}{kT}\frac{\zeta_b(\beta_0)}{(K_s K_0)^{1/2}}\exp\left(\frac{U_0}{kT}\right) \tag{13}$$

$$K_c = \left.\frac{\partial^2 U(h)}{\partial h^2}\right|_{h=0}, \qquad K_s = \left.\frac{\partial^2 U(h)}{\partial h^2}\right|_{h=N\beta_s}, \qquad K_0 = \left.\frac{\partial^2 U(h)}{\partial h^2}\right|_{h=N\beta_0},$$

where $\tau_{c\to s}$ and $\tau_{s\to c}$ are the transition times through the effective potential barrier U_0 from coiled state to stretched one and back, β_0 is the coordinate of the barrier top U_0.

TABLE III
The transition times $\tau_{c\to s}$ and $\tau_{s\to c}$ through the effective potential barrier

	$\tau_{c\to s}$			$\tau_{s\to c}$		
		simulation			simulation	
N	Kramers formulas (13)	1D model	3D model	Kramers formulas (13)	1D model	3D model
50	3.2×10^4	2.1×10^4	1.7×10^4	3.2×10^4	3.1×10^4	2.2×10^4
100	1.9×10^5	2.0×10^5	2.2×10^5	2.3×10^5	2.5×10^5	2.5×10^5
150	1.1×10^6	1.3×10^6	1.5×10^6	1.5×10^6	1.6×10^6	1.8×10^6
200	6.5×10^6	6.9×10^6	6.8×10^6	8.9×10^6	9.2×10^6	7.9×10^6
250	3.7×10^7	4.3×10^7	5.0×10^7	5.3×10^7	7.0×10^7	6.3×10^7

Denominator 2 in (12) is related with nonsymmetry about $\beta = 0$ of the effective potential well, corresponding to unstretched dumbbells (see Figure 1). Thus in the case of equal K_c and K_s slopes of potential the wells, the weight of the stretched state must be twice as large as that of the unstretched state. From simulation the transition times were obtained with the help of the technique proposed by Helfand.[15] When the dumbbell approached the vicinity of one of the minima $|\beta_{c,s} - \beta| \leq 0.01$ a clock was turned on. The time was calculated until the dumbbell occurs in the vicinity of another minimum. Thereafter the clock was turned to zero and the time was once again until the transition in the opposite direction took place. In this way we can obtain the array of transition times from the coiled to the stretched state and in the opposite direction. According hazard plot technique[15] this array enabled us determine to for every N the average transition times $\tau_{c\to s}$ and $\tau_{s\to c}$ through the potential barrier.

Table III compares the simulated values of $\tau_{c\to s}$ and $\tau_{s\to c}$ for one-dimensional and three-dimensional dumbbell model with those calculated according to the Kramers formulas (12) and (13). There is a good agreement between the simulation results and those predicted for both dumbbell models. The corresponding dependencies $\ln \tau_{s\to c}$ on barrier U_0 are shown in Figure 7. The deviations of simulated results from the Kramers formulas are connected with its inapplicability at low U_0.

Therefore the question about the kinetic properties posed above could also be answered affirmatively.

Nonstationary case

In this part we have studied the evolution of distribution function from the initial coiled or stretched state. We have simulated the dumbbell model with $N = 100$ at different values of velocity gradient $\dot{\epsilon}_{\pm i} = \dot{\epsilon}_{cr} \pm i\Delta\dot{\epsilon}$, $i = 0, 1 \ldots 4$, $\dot{\epsilon}_{cr} = 3.818 \times 10^{-4}$, $\Delta\dot{\epsilon} = 0.062 \times 10^{-4}$. At $t = 0$, $\boldsymbol{h} = (20, 0, 0)$ (coiled state) or $\boldsymbol{h} = (70, 0, 0)$ (stretched state). The corresponding effective potential curves $U(\beta)$ are presented in Figure 1 for some values of $\dot{\epsilon}$. For every initial condition and every velocity gradient value 50 runs were performed and distribution functions $\Psi(\beta, n)$ over all runs at every time interval from $t_{n-1} = (n-1)80\Delta t$ to $t_n = n80\Delta t$ $(n = 1, 2, 3 \ldots)$ were calculated. With the help of $\Psi(\beta, n)$ the average extension ratios $\langle\beta(n)\rangle$ of the dumbbell were determined. For every case we have also calculated the transition times τ_{tr} through the corresponding potential barrier using the Kramers formulas (12) and (13). In Figure 8 the dependencies

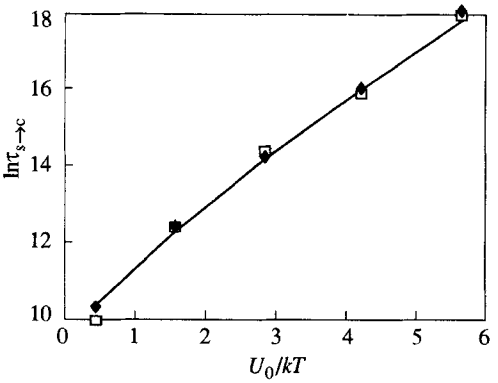

FIGURE 7 The logarithm dependence of transition time $\tau_{s\to c}$ on the barrier height U_0 for 1D model (♦) and 3D model (□).

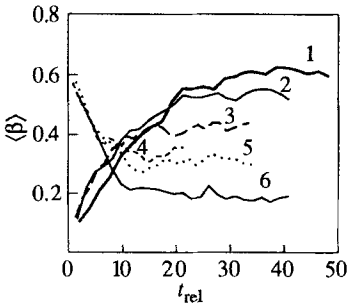

FIGURE 8 The dependence of average extension ratio $\langle\beta\rangle$ on $t_{rel} = t/\tau_{tr}$ for different $\dot{\epsilon}$. Curves 1–3 obtained from the initial coiled state, curves 4–6 obtained from the initial stretched state of the dumbbell. $\dot{\epsilon} = 4.005 \times 10^{-4}$ (curve 1), $\dot{\epsilon} = 3.943 \times 10^{-4}$ (curve 2), $\dot{\epsilon} = 3.880 \times 10^{-4}$ (curve 3), $\dot{\epsilon} = 3.818 \times 10^{-4}$ (curve 4), $\dot{\epsilon} = 3.756 \times 10^{-4}$ (curve 5), $\dot{\epsilon} = 3.693 \times 10^{-4}$ (curve 6).

of average extension ratio on time t_{rel} expressed in units of τ_{tr} for some values of velocity gradient and for two initial conditions (coiled and stretched states) are presented. One can see that at large t_{rel} the values of $\langle\beta\rangle$ stop to change. The dependence of stationary values of $\langle\beta\rangle$ on $\dot{\epsilon}$ is a single valued curve (see Figure 9) as the curves obtained by Bird *et al.*[16] But if dependencies of $\langle\beta\rangle$ on $\dot{\epsilon}$ are plotted at low t_{rel} we obtain the S-shaped curves similar to those of de Gennes.[4]

Therefore the de Gennes approach is correct at observation times comparable with the times of transition through the effective potential barriers. This is what usually occurs at real experimental situation.[6] To obtain the S-shaped curve Bird should have solved the diffusion equation with initial conditions corresponding to both coiled and stretched states and he should have considered nonstationary solutions.

5. CONCLUSION

Thus the simulation by the Brownian dynamics technique was first used investigation of the coil-stretched chain transition of flexible polymers in an elongational flow. The comparison of the simulation results with those obtained analytically by effective potential

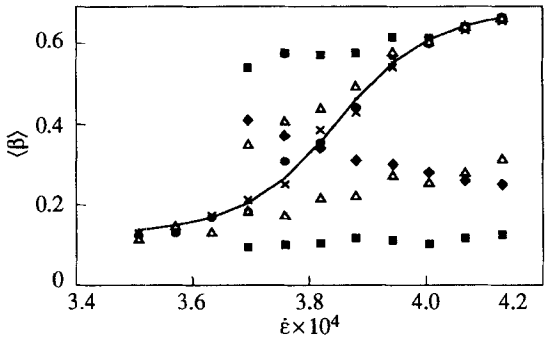

FIGURE 9 The dependence of $\langle\beta\rangle$ on the velocity gradient $\dot{\epsilon}$ for the stationary case: analytical results (solid curve), simulation results for transition from coiled (×) and stretched (●) initial states. For the nonstationary case: $t_{rel} = 5$ (Δ) and $t_{rel} = 1$ (■). The β values corresponding to barrier tops U_0 are represented by (♦). Manually drawn S-shaped curve connecting (♦) and (●) resembles that of de Gennes.

approximation showed that the later correctly describes the equilibrium properties of the system. The transition times through the effective potential barrier were in good agreement with the prediction of the Kramers theory for the motion of the Brownian particle over the one-dimensional potential barrier. Some points of the discussion between Bird and de Gennes are clarified.

References

1. J. A. Odell and A. Keller, *Polymer*, **26,** 1219 (1985).
2. J. A. Odell and A. Keller, *J. Polym. Sci., Polym. Phys. Ed.*, **24,** 1889 (1986).
3. Yu. V. Brestkin, *Acta Polymerica*, **38,** 5470 (1987).
4. P. de Gennes, *J. Chem. Phys.*, **60,** 5030 (1974).
5. Yu. V. Brestkin, Yu. Ya. Gotlib, and L. I. Klushin, *Vysokomol. Soedinen.*, **A31,** 1704 (1989).
6. Yu. Ya. Gotlib and L. I. Klushin, *Vysokomol. Soedinen.*, **A32,** 273 (1990).
7. X.-J. Fan, R. B. Bird, and M. Renardy, *J. Non-Newtonian Fluid Mech.*, **18,** 255 (1985).
8. R. B. Bird, C. F. Curtiss, R. C. Armstrong, and O. Hassager, *Dynamics of Polymeric Liquids, Kinetic Theory* (Wiley-Interscience, New York, 1987), 2nd ed. Chap. 10, p. 471.
9. G. G. Fuller and L. G. Leal, *J. Non-Newtonian Fluid Mech.*, **8,** 271 (1981).
10. N. Phan-Thien, O. Manero, and L. G. Leal, *Rheologica Acta*, **23,** 151 (1984).
11. Yu. Ya. Gotlib, L. I. Klushin, and Yu. Ye. Svetlov, *Vysokomol. Soedinen.*, **A31,** 1049 (1989).
12. Yu. V. Brestkin, Yu. Ya. Gotlib, and L. I. Klushin, *Vysokomol. Soedinen.*, **A31,** 1143 (1989).
13. M. Fixman, *Macromolecules*, **19,** 1195 (1986).
14. S. Chandrasekhar, *Rev. Mod. Phys.*, **15,** 1 (1943).
15. E. Helfand, *J. Chem. Phys.*, **69,** 1010 (1978).
16. J. M. Wiest, L. E. Wedgewood, and R. B. Bird *J. Chem. Phys.*, **90,** 587 (1989).